"Perfect" Electrochemical Molecular Sieving by Thin and Ultrathin Metallopolymeric Films

Suzanne Bélanger, Keith J. Stevenson, Shikata A. Mudakha, and Joseph T. Hupp*

Department of Chemistry and Materials Research Center, Northwestern University, Evanston, Illinois 60208

Received July 17, 1998. In Final Form: November 25, 1998

Oxidative electropolymerization at glassy carbon and indium−tin−oxide electrodes from unbuffered aqueous solutions of $Fe(5\text{-}NH_2\text{-}phen)_3^{2+}$ and $Ru(5\text{-}NH_2\text{-}phen)_3^{2+}$ yields electrode-supported films that self-limit at thicknesses of ca. 50 and 2 nm, respectively. Electrodeposition is characterized by formation of nonelectroactive films, which are electronically insulating at least over the electrochemical potential range of 0 to +1 V. Electrochemical measurements of redox-active probe molecules demonstrate that these films exhibit highly selective molecular sieving. Neutral permeants and hydrophobic permeants are observed to penetrate the polymeric coating more rapidly than charged or hydrophilic forms. Atomic force microscopy, UV−vis spectroscopy, and X-ray photoelectron spectroscopy were used to correlate the polymeric molecular structure with the observed electrochemical reactivity. Molecular sieving behavior is discussed in terms of a membrane transport model implying that the films are comprised of metallopolymeric molecular cavities of uniform size and distribution.

Introduction

Electrochemically synthesized metallopolymeric films[1] have attracted considerable attention in the contexts of chemical sensing,[2] electrocatalysis,[3] electrochromism,[4] and fundamental electron transport/materials conductivity investigations.[5] We have been particularly interested in size- and shape-selective molecular and ionic transport through such films: In principle, optimization of these properties, together with binding properties, can contribute tremendously to the chemical specificity achievable in the aforementioned applications, as well as in applications such as membrane-based ultrafiltration and separator-controlled fuel cell optimization. An interesting and ubiquitous trade-off in almost all transport-related applications concerns film or membrane thickness optimization. Thicker films offer greater mechanical stability and usually contain fewer pinhole-type defects; thus, they tend to provide superior permeant size and shape discrimination.[6] Thinner films, on the other hand, permit larger transport fluxes. Indeed, permeant fluxes generally scale inversely with film thickness.[7] Thus, ultrathin films—if they could be prepared and retained in defect-free form—should be capable of sustaining exceedingly high, chemically selective, permeant transport rates.

One approach to selective transport optimization is to prepare films of moderate or low thickness and then plug pinholes in a subsequent film patching step. We have been exploring this approach in transport studies involving thin films of channel forming "molecular square" compounds.[8,9] Borrowing an idea from the self-assembled monolayer literature,[10] we have been preparing films on conductive electrode platforms and then plugging pinholes by electrochemically polymerizing comparatively large (i.e., channel excluded) transition-metal complexes at the exposed electrode/solution sites. As part of the study, we have also examined the transport/blocking behavior of the patching material itself on naked electrode surfaces. For the materials chosen—films derived from oxidative polymerization of tris(5-amino-1,10-phenanthroline) metal complexes (shown below) in water[11]—we have encountered behavior and responses that are interesting in their own right. Most notably, we find that self-limiting metallopolymer film growth occurs and that the limiting behavior leads to apparently pinhole-free film formation—even for ultrathin films—as evidenced by electrochemical

(1) For reviews, see: (a) Murray, R. W. *Annu. Rev. Mater. Sci.* **1984**, *14*, 145. (b) Abruña, H. D. *Coord. Chem. Rev.* **1988**, *86*, 135.

(2) Representative work: (a) Frew, J. E.; Hill, H. A. O. *Anal. Chem.* **1987**, *59*, 933A. (b) Amos, L. J.; Duggal, A.; Mirsky, E. J.; Ragonesi, P.; Bocarsly, A. B. *Anal. Chem.* **1988**, *60*, 245. (c) Heller, A. *J. Phys. Chem.* **1992**, *96*, 3579. (d) Natan, M. J.; Wrighton, M. S. *Prog. Inorg. Chem.* **1989**, *37*, 391.

(3) Representative work: (a) Buttry, D. A.; Anson, F. C. *J. Am. Chem. Soc.* **1984**, *106*, 59. (b) Guadalupe, A. R.; Usifer, D. A.; Potts, K. T.; Hurrell, H. C.; Mogstad, A. E.; Abruña, H. D. *J. Am. Chem. Soc.* **1988**, *110*, 3462. (c) Andrieux, C. P.; Haas, O.; Savéant, J. M. *J. Am. Chem. Soc.* **1986**, *108*, 8175. (d) Stoessel, S. J.; Elliot, C. M.; Stille, J. K. *Chem. Mater.* **1989**, *1*, 259. (e) O'Toole, T. R.; Meyer, T. J.; Sullivan, B. P. *Chem. Mater.* **1989**, *1*, 574. (f) Nishihara, H.; Pressprich, K., Murray, R. W.; Collman, J. P. *Inorg. Chem.* **1990**, *29*, 1000.

(4) See, for example: (a) Elliot, C. M.; Redepenning, J. G. *J. Electroanal. Chem.* **1986**, *197*, 219. (b) O'Toole, T. R.; Sullivan, B. P.; Meyer, T. J. *J. Am. Chem. Soc.* **1989**, *111*, 5699. (c) Zhang, H.-T.; Subramanian, P.; Fussa-Rydel, O.; Bebel, J. C.; Hupp, J. T. *Sol. Energy Mater.* **1992**, *25*, 315.

(5) See, for example: (a) Chidsey, C. E. D.; Murray, R. W. *J. Phys. Chem.* **1986**, *90*, 1479. (b) Chidsey, C. E. D.; Murray, R. W. *Science* **1986**, *231*, 25. (c) Chidsey, C. E. D.; Luiacono, D. N. *Langmuir* **1990**, *6*, 682.

(6) Pinholes are defined here as trans membrane defects of ca. micrometer lateral dimension, i.e., small compared with film or membrane lateral dimensions, but large compared with isolated molecules and ions. They are particularly insidious in transport applications because they tend to afford much higher area-normalized fluxes than do the films themselves. A comparatively small number of pinholes, therefore, can yield chemically indiscriminate molecular or ionic fluxes that exceed the chemically selective fluxes (overall fluxes) provided by the film or membrane itself.

(7) Baker, R. W.; Cussler, E. L.; Eykamp, W.; Koros, W. J.; Riley, R. L.; Stathmann, H. *Membrane separation systems. Recent developments and future directions*; Noyes Data Corporation: Park Ridge, 1991.

(8) (a) Slone, R. V.; Benkstein, K. D.; Bélanger, S.; Hupp, J. T.; Guzei, I. A.; Reingold, A. L. *Coord. Chem. Rev.* **1998**, *171*, 221. (b) Bélanger, S.; Hupp, J. T.; Stern, C. L., Slone, R. V.; Watson, D. F.; Carrell, T. M. Manuscript in preparation.

(9) See also: Stang, P. J.; Olenyuk, B. *Acc. Chem. Res.* **1997**, *30*, 502 and references therein.

(10) (a) Finklea, H. O.; Snider, D. A.; Fedyk, J. *Langmuir* **1990**, *6*, 371. (b) Rubinstein, I.; Steinberg, S.; Tor, Y.; Shanzer, A.; Sagiv, J. *Nature* **1988**, *332*, 426.

10.1021/la980908r CCC: $18.00
Published on Web 12/31/1998

molecular sieving experiments. We note that qualitatively similar behavior has been described previously based on insulating organic film formation via irreversible oxidation of phenol and related compounds.[12,13] The key difference is that the size cutoff for molecular permeant transport is much larger for films derived from the transition-metal complexes. In the sections that follow, we report on the synthesis, electrochemical characterization, and physical characterization of the metallopolymer films, and illustrate the apparently perfect electrochemical molecular sieving characteristics of thin (≤50 nm) and ultrathin (∼2 nm) versions of the films.

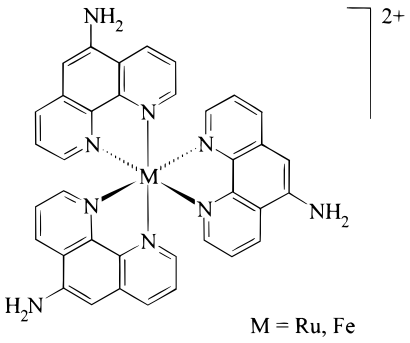

Experimental Section

Materials. $[Fe(5\text{-}NH_2\text{-}phen)_3](PF_6)_2$ and $[Ru(5\text{-}NH_2\text{-}phen)_3](PF_6)_2$ (5-NH_2-phen = 5-amino-1,10-phenanthroline) were prepared as described for related complexes.[14] 5-Amino-1,10-phenanthroline was purchased from Polysciences, Inc. $[Ru(NH_3)_5(4\text{-}pic)](PF_6)_2$ (4-pic = 4-picoline = 4-methylpyridine) was prepared as described previously;[15] $[Ru(NH_3)_5(4\text{-}phpy)](PF_6)_2$ (4-phpy = 4-phenylpyridine) was prepared via the same method. $[Co(bpy)_3](NO_3)_2$ (bpy = 2,2?-bibyridine) and $[Co(phen)_3](NO_3)_2$ (phen = 1,10-phenanthroline) were prepared from $Co(NO_3)_2 \cdot 6H_2O$ in ethanol as described in the literature for the perchlorate analogues.[16] Ferrocenemethanol (FcMeOH) was purchased from Aldrich, and (trimethylammonio)methylferrocenium tetrafluoroborate ($[Fc-CH_2-N(CH_3)_3](BF_4)$) was prepared as described elsewhere.[17] All other permeants and solvents were obtained from Aldrich. Aqueous solutions were prepared by using water obtained from a water purification system (Barnstead Millipore) fed by an in-house distilled water line.

Surface Characterization. Atomic force microscopy was performed by using a Digital Instruments Multimode Nanoscope IIIa. All measurements were obtained in tapping mode with single etched silicon (TESP) Nanoprobe SPM tips (cantilever length 125 μm and resonance frequency 307−367 Hz, Digital Instruments). Estimates of electrodeposited film thickness were obtained from atomic force microscopy (AFM) images of the indium−tin−oxide (ITO)/poly-$[Fe(5\text{-}NH_2\text{-}phen)_3^{2+}]$ boundary using the "section analysis" function of the Digital Nanoscope software (version 4.23r2). X-ray photoelectron spectroscopy (XPS) data were obtained at the University of Utah by using a VG ESCA lab 220i multianalyzing instrument with Al Kα radiation of 1486.7 eV and an electron takeoff angle of 90° with respect of the sample surface. The X-ray gun (200-μm spot size) was positioned at 45° with respect to the entrance axis of the hemispherical kinetic energy analyzer. The pass energy for survey scans was set to 100 eV while that for high-resolution scans was set to 20 eV. The binding energy was calibrated with respect to the C 1s binding energy of 284.6 ± 0.1 eV.

Electrochemical Measurements. Voltammetric measurements were made by using a Princeton Applied Research polarographic analyzer (model 264A) and a Houston Instruments XY recorder. Disk electrode rotation was accomplished with a Pine Instruments analytical rotator (model MSRX). A one-compartment, three-electrode cell was used for the electrochemical measurements. Pt wire and Ag/AgCl (BAS, 3 M NaCl) were employed as the counter and reference electrodes, respectively. Except where noted otherwise, all rotating disk electrode (RDE) voltammetry measurements utilized 3 mm diameter glassy carbon (GC) disk working electrodes (BAS). Rotation rates typically varied from 10 to 1000 rpm in the permeation studies. Films for electronic absorption spectral measurements were obtained using ITO-coated glass (Delta Technologies, Ltd., 10 Ω/square) as a working electrode material.

Results and Discussion

Mechanism of Oxidative Electropolymerization. The mechanism involved in the formation of poly-$[M(5\text{-}NH_2\text{-}phen)_3]^{2+}$ (M = Fe, Ru) and poly-(5-NH_2-phen) has been described previously.[11b,d] Briefly, oxidation of an amine substituent on the phenanthroline generates a ligand-bound radical cation ($NH_2 \rightarrow NH_2^{\bullet+}$), which subsequently loses a proton to give a neutral radical ($NH_2^{\bullet+} \rightarrow NH^{\bullet}$). This radical either can combine with another $NH^{\bullet}$ radical to form a diazo linkage or can attack a carbon atom of a second phenanthroline ligand and form an imine linkage. Although these two oxidation steps are not usually resolved,[11b,c,e,f] two distinct waves have previously been reported for the ligand oxidation.[11a,d] The aforementioned polymerization chemistry clearly is similar to that entailed in polyaniline formation.[11b,18] In contrast to polyaniline, however, the metallopolymers are essentially electronically insulating. The insulating behavior is an expected consequence of the pseudo-octahedral coordination of 5-aminophenanthroline by the metal centers: by configuring trios of ligands orthogonally, the metal ions preclude the creation of the extended planar aromatic structures required for electronic conduction in materials of this kind. On the other hand, as Ellis and co-workers have pointed out,[11b] the availability of an electroactive metal center does provide a basis for *redox* conductivity (mixed-valent electron hopping type conductivity). If the redox potential equals or exceeds that associated with amine substitutent oxidation, sustained polymer growth becomes possible. Conversely, if metal-centered redox reactions could be avoided, self-limiting metallopolymer growth and ultrathin film formation might be envisioned.

Electropolymerization of $Ru(5\text{-}NH_2\text{-}phen)_3^{2+}$. Voltammetric cycling of either a GC disk electrode or an ITO electrode between 0.5 and 1.2 V in an aqueous solution containing ∼0.3 mM $Ru(5\text{-}NH_2\text{-}phen)_3^{2+}$ (solubility limit) and 0.25 M KNO_3 yields an irreversible oxidation wave that peaks at +0.8 V. From prior work,[11d] the wave is

(11) (a) Chen, S.-M. *J. Electroanal. Chem.* **1996**, *401*, 147. See also: (b) Ellis, C. D.; Margerum, L. D.; Murray, R. W.; Meyer, T. J. *Inorg. Chem.* **1983**, *22*, 1283. (c) Pickup, P. G.; Osteryoung, R. A. *Inorg. Chem.* **1985**, *24*, 2707. (d) Nyasulu, F. W. M.; Mottola, H. A. *J. Electroanal. Chem.* **1988**, *239*, 175. (e) Yan, S. G.; Hupp, J. T. *J. Electroanal. Chem.* **1995**, *397*, 119. (f) Bachas, L. G.; Cullen, L.; Hutchins, R. S.; Scott, D. L. *J. Chem. Soc., Dalton Trans.* **1997**, 1571. (g) de Gregori, I.; Bedioui, F.; Devynck, J. *J. Electroanal. Chem.* **1987**, *238*, 197.

(12) (a) Ohnuki, Y.; Matsuda, H.; Ohsaka, T.; Oyama, N. *J. Electroanal. Chem.* **1983**, *158*, 55. (b) Ohsaka, T.; Hirokawa, T.; Miyamoto, H.; Oyama, N. *Anal. Chem.* **1987**, *59*, 1758. (c) Taj, S.; Ahmed, M. F.; Sankarapapavinasam, S. *Indian J. Chem.* **1993**, *32A*, 521. (d) McCarley, R. L.; Irene, E. A.; Murray, R. W. *J. Phys. Chem.* **1991**, *95*, 2492.

(13) (a) Lane, R. F.; Hubbard, A. T. *J. Phys. Chem.* **1973**, *77*, 1401. (b) Lane, R. F.; Hubbard, A. T. *J. Phys. Chem.* **1973**, *77*, 1411.

(14) Fussa-Rydel, O.; Zhang, H.-T.; Hupp, J. T.; Leidner, C. R. *Inorg. Chem.* **1989**, *28*, 1533.

(15) Curtis, J. C.; Sullivan, B. P.; Meyer, T. J. *Inorg. Chem.* **1983**, *22*, 224.

(16) Wheeler, S. H.; Zingheim, S. C.; Nathan, L. C. *J. Inorg. Nucl. Chem.* **1978**, *40*, 779.

(17) Nielson, R. M.; Lyon, L. A.; Hupp, J. T. *Inorg. Chem.* **1996**, *35*, 970.

(18) See, for exemple: (a) Breitenbach, M.; Heckner, K. H. *J. Electroanal. Chem.* **1971**, *29*, 309. (b) *Organic Electrochemistry: an Introduction and Guide*, 3rd ed.; Lund, H., Baizer, M. M., Eds.; Marcel Dekker: New York, 1991; p 587. (c) Volkov, A.; Tourillon, G.; Lacaze, P.-C., Dubois, J.-E. *J. Electroanal. Chem.* **1980**, *115*, 279.

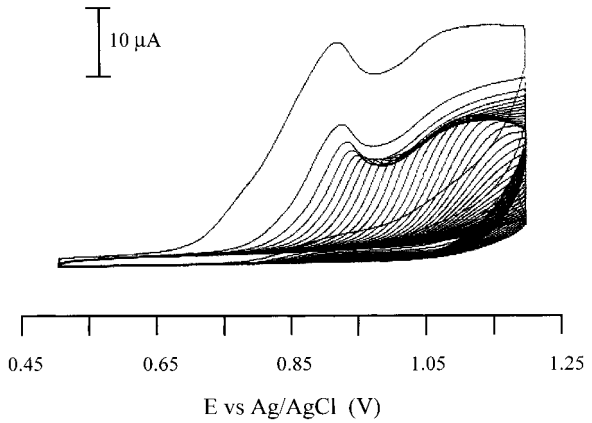

Figure 1. Repetitive volumetric response of a GC disk electrode (diameter = 3 mm) in an aqueous 0.5 mM solution of Fe(5-NH_2-phen)$_3^{2+}$ and 0.25 M KNO_3. Scan rate = 0.1 V/s.

assignable to amine substitutent oxidation. Note that under these conditions, the expected oxidation of Ru(II), at ~1.3−1.4 V, is avoided. Continued cycling diminishes the height of the amine oxidation wave, with electrode passivation occurring after about five cycles. Subsequent (ex situ) height and phase-contrast AFM measurements and related measurements made in air on the ITO/polymer boundary region indicated the presence of an extremely thin (1.6 ± 0.3 nm) hydrophobic coating. While it is difficult to prove unambiguously that the coating is polymeric, the similarity of this behavior to that of thicker poly-[Fe(5-NH_2-phen)$_3^{2+}$] coatings—especially in film permeation experiments (see below)—strongly suggests that it is. Indeed, electrode passivation and ultrathin metallopolymer film formation would be expected if amine oxidation were initiated under conditions where metal-based mediation could not sustain the electrochemical oxidation reaction.

Electropolymerization of Fe(5-NH_2-phen)$_3^{2+}$. Figure 1 shows a representative voltammetric response from a GC disk electrode in contact with an aqueous solution of 0.5 mM Fe(5-NH_2-phen)$_3^{2+}$ and 0.25 M KNO_3 . Here, the initial electrochemical response is dominated by an irreversible oxidative wave peaking at +0.9 V. This wave is believed to be a superimposition of waves for both oxidation of amine substituents and the Fe(II) center (note that three amine groups exist per metal center).[19] A broader voltammetric wave is observed at more positive potentials, which is believed to result from contributions of additional faradaic amine oxidation and the generation of a nonfaradaic charging current, a consequence of the changing interfacial capacitance during polymeric film growth. A qualitatively similar behavior has been reported for the oxidation of the unbound 5-NH_2-phen ligand on carbon paste electrodes,[11d] where the presence of two waves has been attributed to two resolved oxidation steps: formation of the $NH_2^{\bullet+}$ radical (and subsequent proton loss to yield a neutral $NH^{\bullet}$ radical), followed by the formation of diazo or imine linkages. Upon repetitive cycling, a systematic decrease in the anodic current is observed and the peak potential shifts to more positive potentials. This shift is believed to arise from conversion of amine groups to imine or diazo functionalities; these functionalities are substantially more electron withdrawing and are expected, therefore, to stabilize Fe(II) with respect to Fe(III).[11d] (Curiously, the accompanying loss in Fe(II/III) electroactivity can be significantly restored, albeit only transiently, by transferring the coated electrode to a nonhydroxylic solvent such as methylene chloride or acetonitrile.) Despite the decrease in anodic current, polymer growth occurs with each successive cycle, as evidenced by thickness measurements presented below. Similar voltammetric responses are obtained at ITO and Pt electrodes. All films formed (more than five voltammetric cycles) have a red tint visible to the naked eye.

Electropolymerization of 5-NH_2-phen. The free 5-NH_2-phen ligand is insoluble in unbuffered water but is soluble in highly acidic solution. Oxidative scanning (in the +0.5 to 1.2 V range) of a ligand solution containing 0.2 M aqueous HNO_3 yields an electrochemical behavior that is qualitatively similar to that encountered in unbuffered Ru(5-NH_2-phen)$_3^{2+}$ solutions. Thus, the current, peaking near 1.05 V, decreases significantly during the first few cycles, subsequently stabilizing at about half of the original value after 10 cycles. Further cycling, however, does not lead to passivation of the electrode, and films obtained by oxidative polymerization do not block the electrochemistry of added redox probe species (see below). Cycling in the −1.0 to 1.0 V range, on the other hand, does yield a (presumably polymeric) film, which is fully blocking with respect to $Ru(NH_3)_6^{2+}$ oxidation.

Determination of Film Thickness for Poly-[Fe(5-NH_2-phen)$_3^{2+}$]. For fully redox active polymers, the film thickness (coverage) can be estimated by integration of the faradaic charge passed in the voltammetric response. The loss of electroactivity encountered here, however, prevents estimation of the polymer thickness from electrochemical data. For this reason, tapping mode atomic force microscopy (TMAFM) was used to determine film thickness and characterize the electropolymerized film morphology. Figure 2a shows a 100 × 100 μm TMAFM image of the ITO/poly-[Fe(5-NH_2-phen)$_3^{2+}$] boundary formed at the air/solution interface during oxidative electropolymerization of aqueous Fe(5-NH_2-phen)$_3^{2+}$. On the left side of the boundary is the bare ITO electrode surface and to the right is the electropolymerized film deposited after 40 voltammetric cycles. Figure 2a indicates that oxidative electropolymerization produces thin polymeric films of uniform dimensions. Larger polymeric protrusions are also observed within the film. The thickness (determined from the average of five independent measurements) of the polymer film was ~39 ± 3 nm. Figure 2b shows a higher resolution 3 × 3 μm AFM image of the poly-[Fe(5-NH_2-phen)$_3^{2+}$] coating. The morphology is characterized by close packed, irregular domains (bundles) of 60 to 100 nm diameter. The estimated root-mean-square (RMS) surface roughness for this sample was 6 nm. (The RMS roughness of the ITO samples themselves was ca. 4 nm.)

A plot of AFM-determined film thickness versus number of voltammetric cycles is shown in Figure 3. Polymer growth is observed to occur nearly linearly for the first 25 voltammetric cycles. Assuming that one monolayer is ~1.5 nm thick, Figure 3 demonstrates that slightly less than one monolayer is deposited per voltammetric cycle. Additional cycles are less effective, with the film thickness ultimately reaching a limiting value of ~50 nm. This finding is consistent with the electrochemical observation (above) of blockage of monomer oxidation by electrode passivation, after several dozen voltammetric cycles. Similar observations have been reported by Chen[11a] for the oxidative polymerization of Fe(5-NH_2-phen)$_3^{2+}$ in buffered aqueous solution: electropolymerization ceased

(19) The reversible Fe(II/III) couple for the Fe(5-NH_2-phen)$_3^{2+}$ monomer in acetonitrile/$TBAPF_6$, where the polymer growth does not take place, is 0.1 V negative of that of Fe(phen)$_3^{2+}$. The Fe(II/III) redox couple for Fe(phen)$_3^{2+}$ in aqueous KNO_3 is 0.85 V, and, based on this observation, the Fe(II/III) couple for the Fe(5-NH_2-phen)$_3^{2+}$ monomer in water is expected near +0.75 V.

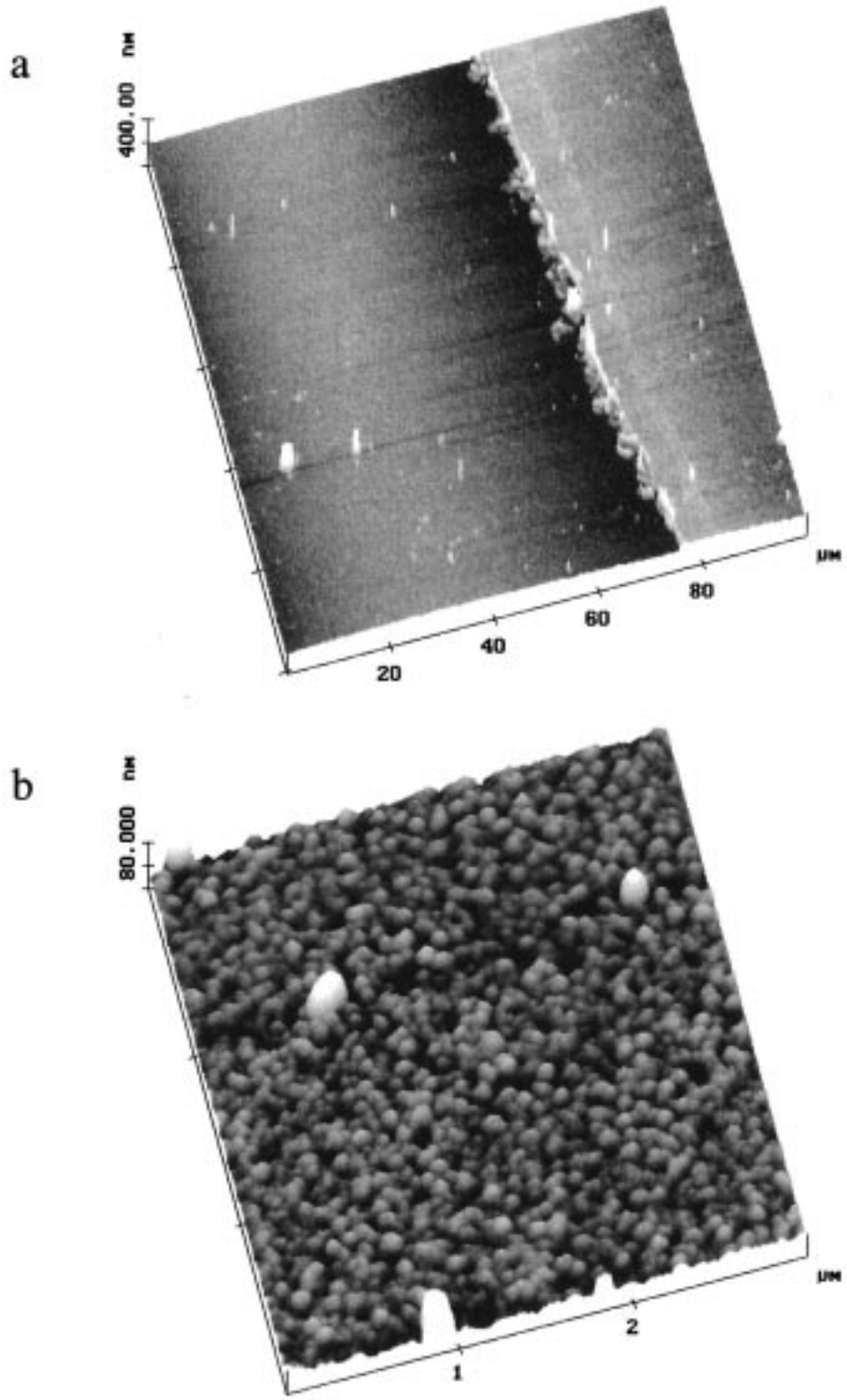

Figure 2. AFM images of a 39 nm thick poly-[Fe(5-NH_2-phen)$_3^{2+}$] film grown on ITO from an aqueous solution of 0.5 mM Fe(5-NH_2-phen)$_3^{2+}$ and 0.25 M KNO_3: (a) 100 × 100 μm height image showing bare ITO/polymer boundary. (b) 3 × 3 μm height image showing poly-[Fe(5-NH_2-phen)$_3^{2+}$] film morphology.

after 50 voltammetric cycles. The correlation shown in Figure 3 was used to estimate thicknesses of films used in RDE-based permeation studies (see below).[20]

The eventual loss of film electroactivity, together with the cessation of redox-mediated (i.e., poly-[$Fe^{III/II}$(5-NH_2-phen)$_3$]) film growth, suggested to us that demetalation might be occurring.[21] One test of this hypothesis would be to compare the Fe^{II}(5-NH_2-phen)$_3^{2+}$ content implied by visible-region film absorption measurements (transparent electrode platforms) with that implied by film thickness measurements. UV−vis spectra of poly-[Fe(5-NH_2-

(20) Additional TMAFM and electrochemical studies conducted on GC and ITO electrodes demonstrated that polymerization of Fe(5-NH_2-phen)$_3^{2+}$ from aqueous solutions yields the same morphology, as shown in Figure 2, regardless of the electrode substrate used.

(21) Evidence for a dimeric hydroxo-bridged Fe(III) hydrolysis product resulting from loss of phenanthroline ligand has been reported previously.[11a]

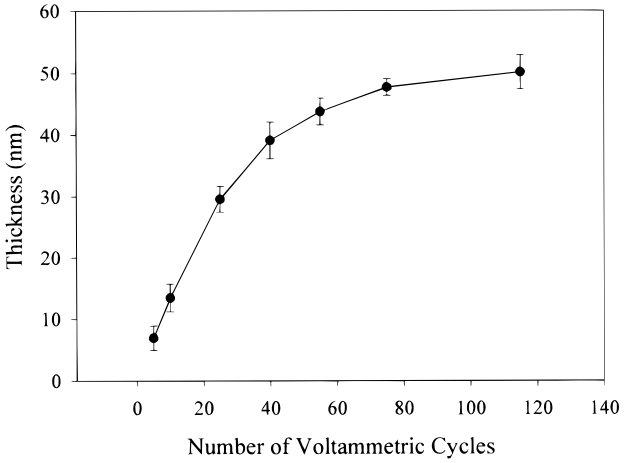

Figure 3. Plot of AFM-measured film thickness versus number of voltammetric cycles for poly-[$Fe(5\text{-}NH_2\text{-}phen)_3^{2+}$] film growth.

$phen)_3^{2+}$]/ITO electrodes show a distinct absorption band at 520 nm, as expected and reported previously.[11a,c] Assuming that close packing occurs and that each intact monomer unit occupies a sphere of 16 Å diameter, and assuming that the monomer oscillator strength is not changed by polymer incorporation, the absorbance experiments indicate that at least half the available coordination sites remain metalated. If less dense packing is assumed, then an even higher metal retention (perhaps even complete retention) is indicated.

X-ray photoelectron spectroscopy was also used to examine polymer film compositions (both elemental composition and metal oxidation state). XPS spectra for poly-[$Fe(5\text{-}NH_2\text{-}phen)_3^{2+}$] and solvent-evaporated monomer samples on ITO electrodes show an intense signal at 709.0 eV. The observed binding energy is within the range of Fe $2p_{3/2}$ binding energies (708−710 eV) previously reported for oxygen- and carbon-bound iron(II) complexes.[22] The absence of a $2p_{3/2}$ signal at higher binding energy (711−712 eV), expected for iron(III) complexes, suggests that most or all of the polymer-bound iron exists in oxidation state II. An attempt to quantify the iron content was made by comparing iron-to-carbon ratios for polymer samples with that for monomer (relative ratios obtained by integrating relative XPS intensities).[23] Assuming a 1:36 Fe:C ratio for $Fe(5\text{-}NH_2phen)_3^{2+}$ monomer, XPS spectra yield roughly 1:50 Fe:C ratios for polymeric samples. We conclude, therefore, that demetalation does not occur extensively and, thus, does not account for the observed loss of electroactivity.

Permeation Measurements: Molecular Sieving. Films prepared by electropolymerization of $Fe(5\text{-}NH_2\text{-}phen)_3^{2+}$ exhibit seemingly perfect molecular sieving behavior, suggesting that exceptionally thin (2−3 nm, two polymerization cycles) and remarkably defect-free coatings can be prepared. This is illustrated in Figure 4, which compares voltammetric responses for two redox-active permeants, $Ru(NH_3)_6^{2+}$ and $Co(phen)_3^{2+}$, at a bare GC electrode, and at an electrode covered with less than two molecular layers (two polymerization cycles) of poly-[$Fe(5\text{-}NH_2\text{-}phen)_3^{2+}$]. The experiments show that the film is

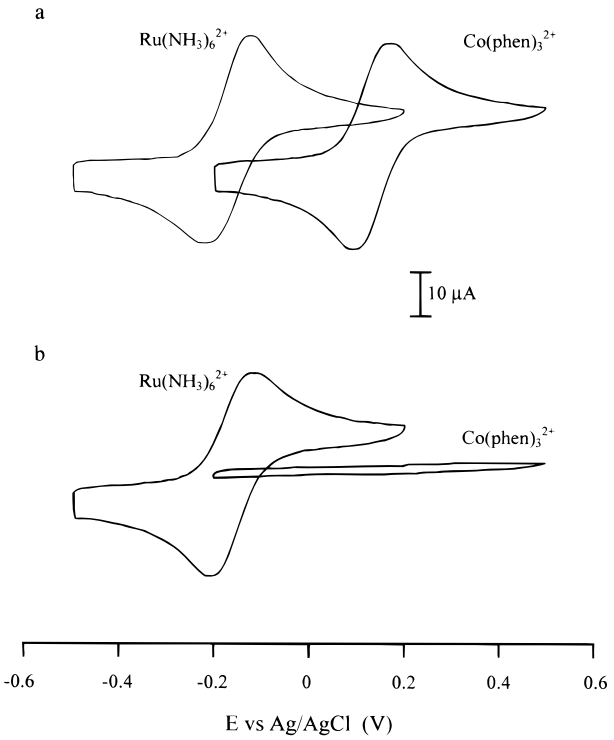

Figure 4. Voltammetric response of (a) uncoated and (b) poly-[$Fe(5\text{-}NH_2\text{-}phen)_3^{2+}$]-coated GC disk electrode (diameter = 3 mm) in an aqueous solution of 0.5 M KNO_3 and 2.6 mM $Co(phen)_3^{2+}$, and an aqueous solution of 0.5 M KNO_3 and 2.3 mM $Ru(NH_3)_6^{2+}$. Scan rate = 0.1 V/s.

permeable to the smaller Ru species (average diameter (d) ∼ 5.5 Å) but that the larger Co complex (d ∼ 13 Å) is completely excluded from the film. Even thinner films, prepared by cycling the potential once in the +0.5−1.2 V range, exhibited partial molecular sieving, demonstrated by a small residual current (∼10% of the bare electrode current) for $Co(phen)_3^{2+}$. Presumably, this is caused by transport through defects or gaps much larger than molecular dimensions. Within the limited set examined, the smallest probe molecule excluded from poly-[$Fe(5\text{-}NH_2\text{-}phen)_3^{2+}$] films, based on cyclic voltammetry, is $Co(bpy)_3^{2+}$ (d ∼ 11 Å) (experiment not shown). In contrast, probe molecules having diameters of roughly 8 Å or less readily permeate the films. As discussed further below, permeation occurs regardless of molecular charge type.

Thin films obtained by cycling an aqueous solution of $Ru(5\text{-}NH_2\text{-}phen)_3^{2+}$ also show molecular sieving behavior, with a size cutoff identical to that observed for the Fe polymer. However, since polymer growth is limited to a few cycles, thicker films suitable for quantitative permeation studies (see below) were not possible.

In contrast to the two Fe and Ru metallopolymers, thin films prepared by cycling an acidic solution containing the metal-free 5-NH_2-phen ligand between −1.0 and 1.2 V are observed to totally exclude $Co(phen)_3^{2+}$, $Ru(NH_3)_6^{2+}$, and $Ru(NH_3)_6^{3+}$. This observation is consistent with the available permeability data for other electrochemically synthesized organic (polyaromatic) films (e.g., polyphenol, polyaniline, poly(4,4′-diaminophenylester, poly(1,2-diaminobenzene), poly(2,6-dimethyl-1,4-phenylene oxide), poly(*m*-bromophenol)).[12] These materials generally exclude complex ions such as $Fe(edta)^-$ and $Fe(CN)_6^{4-}$ but do display permeability toward extremely small ions such as H^+ and Br^-. The current studies clearly indicate that the presence of the metal ion in $M(5\text{-}NH_2\text{-}phen)_3^{2+}$ complexes allows for the formation of much more porous

(22) (a) Moulder, J. F.; Stickle, W. F.; Soble, P. E.; Bomben, K. D. In *Handbook of X-ray Photoelectron Spectroscopy*; Chastain, J., King, R. C., Eds.; Physical Electronics, Inc.: Eden Prairie, MN, 1995. (b) Umaña, M.; Rolison, D. R.; Nowak, R.; Daum, P.; Murray, R. W. *Surf. Sci.* **1980**, *101*, 295.

(23) Since polymerization of $Fe(5\text{-}NH_2\text{-}phen)_3^{2+}$ was performed in aqueous solutions employing KNO_3 as the supporting electrolye, no attempts were made to determine the iron-to-nitrogen ratio.

Table 1. Comparison of the Permeation Rates in Poly-[Fe(5-NH_2-phen)$_3$]$^{2+}$

	$D_s \times 10^6$ (film covered electrode)[a]	$D_s \times 10^6$ (bare electrode)	$PD_f \times 10^9$ [b]	av diameter of permeant (Å)
$[Ru(NH_3)_6]^{3+}$	16 ± 3	14.7	8.6 ± 1.5	5.5
$[Ru(NH_3)_6]^{2+}$	7.9 ± 0.6	6.0	11 ± 3	5.5
$[Ru(NH_3)_5(4\text{-pic})]^{2+}$	6.7 ± 0.7	6.6	7 ± 1.2	6.7
$[Ru(NH_3)_5(4\text{-phpy})]^{2+}$ [c]	22 ± 10	7.3	3.8 ± 1.0	8.0
$[Fe(CN)_6]^{3-}$	8.9 ± 0.3	7.7	19 ± 4	6.0
$[Fe(CN)_6]^{4-}$	7.3 ± 1.1	7.1	2.6 ± 1.0	6.0
FcMeOH	11.8 ± 0.3	9.6	61 ± 7	4.5
$[Fc\text{-}CH_2\text{-}N(CH_3)_3]^{+}$ [d]	8 ± 2	8.0	14 ± 3	5.0

[a] Determined from the slopes of Koutechý−Levich plots. [a,b] Average for four to seven films of thicknesses ranging from 10 to 40 nm, in the linear portion of the $i_{permeation}$ vs $1/d$ plot. [c] Large uncertainties resulting from permeant decomposition. [d] Measured on a gold electrode. (Fouling occurred of GC electrodes.)

polymeric structures, even under self-limiting film formation conditions. Presumably, the increased porosity or pore size reflects the inherently larger monomer size in the metallopolymer case, the roughly spherical rather than planar monomer shape, and the need to incorporate multiple, charge-compensating anions of significant volume during film growth.

Permeation Measurements: Transport Parameters. Rotating disk electrode voltammetry was used to quantify the permeability of the Fe(II) metallopolymer toward a series of electroactive probe molecules, using a membrane permeation model. Briefly, this model assumes that permeation through the polymer film can be described as uniform diffusion (via pathways of molecular dimensions) in a membrane with uniform pore size distribution and pore size of molecular dimensions, where the permeant has a diffusion coefficient smaller than that in solution.[24a]

If the membrane diffusion model is valid and chemical and physical complications are absent, the limiting current at a film-covered RDE, is given by[24]

$$(i_{lim})^{-1} = (i_{mass\ transport})^{-1} + (i_{permeation})^{-1} \qquad (1)$$

$$(i_{lim})^{-1} = (0.620nFAD_s^{2/3}\omega^{1/2}\nu^{-1/6}C_s)^{-1} + (nFAPD_fC_s/d)^{-1} \qquad (2)$$

In the equations, n is the number of electrons transferred per permeant, F is the Faraday constant, A is the electrode area, D_s is the diffusion coefficient of the permeant in solution, ω is the rotation rate of the electrode, ν is the kinematic viscosity of the solvent, P is the partition coefficient of the solute ($P = C_f/C_s$), C_f and C_s are, respectively, the solute concentrations in the film and in solution, D_f is the diffusion coefficient of the solute within the film, and d is the film thickness.

For very fast diffusion in a polymeric film, or at a bare electrode, the limiting current obeys the Levich equation (i.e., the permeation term of the above equation is negligible or absent), and a plot of i_{lim} vs $\omega^{1/2}$ (Levich plot) is linear with an intercept of zero. In the presence of a polymeric film which significantly inhibits diffusional transport of the electroactive species to the electrode, the limiting current at high rotation rates (high mass transport rates) becomes unresponsive to further increases in the rotation rate; i.e., negative deviations from the Levich behavior are encountered. The effect of a typical poly-[Fe(5-NH_2-phen)$_3^{2+}$] coating on the limiting (RDE) current for ferrocyanide oxidation is shown in Figure 5; deviations

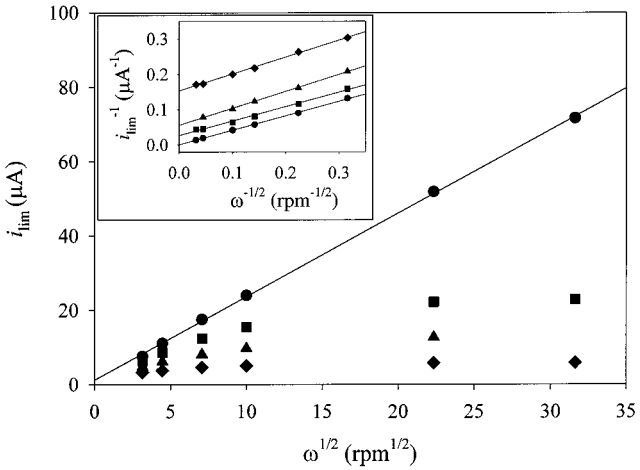

Figure 5. Levich plot (i_{lim} versus $\omega^{1/2}$) for oxidation of $[Fe(CN)_6]^{4-}$ (2.25 mM) at a poly-[Fe(5-NH_2-phen)$_3^{2+}$]-coated GC disk electrode as a function of film thickness. Inset: Koutecký-Levich plot (i_{lim}^{-1} versus $\omega^{-1/2}$). Film thickness (nm): 0 (●), 13 (■), 24 (▲), and 39 (♦).

from simple Levich behavior (solid line) are clearly evident at the highest rotation rates. From eqs 1 and 2, the y-intercept on a i_{lim}^{-1} vs $\omega^{-1/2}$ plot (Koutecký−Levich plot) will yield the film permeation current. The inset in Figure 5 shows that a finite intercept and, therefore, a finite permeation rate are observable for the ferrocyanide/poly-[Fe(5-NH_2-phen)$_3^{2+}$] system.

From eq 2, the permeation current or rate should increase as the film thickness decreases ($i_{permeation} \propto 1/d$). Variable thickness studies involving four to seven films in the 13−39 nm range (10−40 polymerization cycles) were pursued for each of the permeants listed in Table 1. The studies showed, as expected, that thinner films are more permeable and that $i_{permeation}$ is indeed inversely proportional to film thickness. We were optimistic, therefore, that extension of the transport investigation to ultrathin films would yield extremely high permeation currents. Instead, as shown in Figure 6, the thinnest films yielded *smaller* permeation currents (membrane transport rates). This phenomenon has been observed with all permeants studied. An explanation based on annealing was considered, but repetitive scanning showed no changes in current with successive scans. Therefore, we suggest that very thin films may have a less porous structure than thicker ones. We note that annealing behavior has been reported for other systems, but its origin is not well understood.[25] While we have no molecular explanation for the decrease in permeability, comparison of AFM data (not shown) for films of varying thickness (~ 2 to 50 nm) indicates that

(24) (a) Savéant, J.-M. *J. Electroanal. Chem.* **1991**, *302*, 91. (b) Ikeda, T.; Schmehl, R.; Denisevich, P.; Willman, K.; Murray, R. W. *J. Am. Chem. Soc.* **1982**, *104*, 2683. (c) Gough, D. A.; Leypoldt, J. K. *Anal. Chem.* **1979**, *51*, 439. (d) Leddy, J.; Bard, A. J. *J. Electroanal. Chem.* **1983**, *153*, 223. (e) Ewing, A. G.; Feldman, B. J.; Murray, R. W. *J. Phys. Chem.* **1985**, *89*, 1263.

(25) See Pressprich, K. A.; Maybury, S. G., Thomas, R. E.; Linton, R. W.; Irene, E. A.; Murray, R. W. *J. Phys. Chem.* **1989**, *93*, 5568.

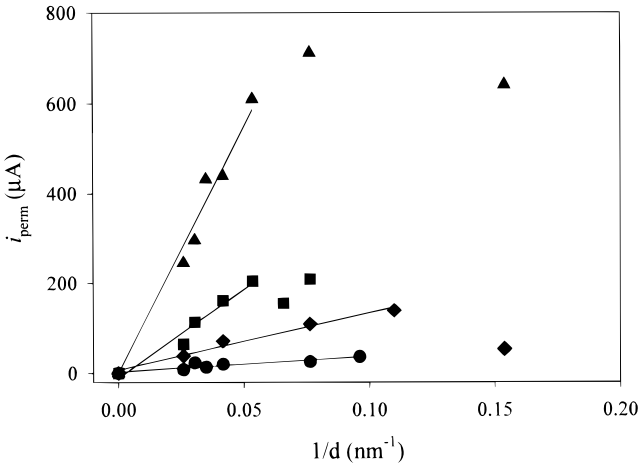

Figure 6. Dependence of permeation current ($i_{permeation}$) versus the reciprocal thickness (d^{-1}) for 0.25 M KNO_3 solutions of $[Fe(CN)_6]^{4-}$ (●), $[Fe(CN)_6]^{3-}$ (■), FcMeOH (▲), and $Ru(NH_3)_63+$ (♦) at a poly-$[Fe(5\text{-}NH_2\text{-}phen)_3^{2+}]$-coated GC disk electrode. Permeation currents normalized to $C_s = 2.5$ mM.

the observed morphology for the thinnest films is clearly different and characterized by nonspherical-shaped, irregular domains of decreased dimensions (20−80 nm).

Comparison of the permeabilities of several electroactive species is made in Table 1 and Figure 6. Perhaps most notable is the exceptionally high relative permeability of ferrocenemethanol ($d \sim 4.5$ Å). While size considerations would suggest a slightly larger film diffusion coefficient for the ferrocenemethanol compound than for the remaining permeants[26] (cf. solution-phase diffusion coefficients in Table 1), the difference is almost certainly insufficient to account for the observed 6- to 8-fold greater permeability for molecules of comparable size. Recall, however, that the permeability depends not only upon the efficacy of film-based diffusion but also upon the degree of solution-to-film partitioning of the permeant.[27] For the metallopolymers, which are comprised of fixed cationic frameworks and exchangeable counteranions, simple electrostatic considerations would suggest large partition coefficients (and, therefore, large permeabilities) for suitably sized anionic permeants, intermediate P values for neutral permeants, and small P values for cationic permeants.[24b,e] The available data clearly argue against a dominant electrostatic effect. We believe instead that the known exceptional hydrophobicity of ferrocene accounts for the evidently extensive partitioning of ferrocenemethanol into the metallopolymeric film.[28] In an effort to distinguish further between contributions due to permeant charge and hydrophilicity, the film permeability of a cationic ferrocene derivative, $Fc\text{-}CH_2\text{-}N(CH_3)_3^+$ was examined. The PD_f (1.4×10^{-8} cm^2/s) is smaller, by a factor of 4, than that of the uncharged ferrocenemethanol species (see Table 1).

On the other hand, for the series of ruthenium-containing permeants, the modest variations in PD_f indicate that size/steric effects outweigh changes in relative hydrophilicity/hydrophobicity. (For example, the most hydrophobic but most sterically demanding ruthenium permeant, $Ru(NH_3)_5(4\text{-phpy})^{2+}$, exhibits the lowest PD_f value.) Finally, a rather remarkable difference in film permeability was encountered for ferricyanide versus ferrocyanide. The observed greater permeability for the latter is inconsistent with a simple electrostatic partitioning interpretation. The unexpected observation was corroborated, however, by measurements indicating a −0.04 to −0.07 V shift in the $Fe(CN)_6^{3-/4-}$ half-wave potential at film-covered electrodes in comparison to a bare electrode. (The expected shift ($E_{1/2,perm} - E_{1/2,bare}$) is $(RT/nF)\ln(P_{red}D_{f,red}/P_{ox}D_{f,ox})$, i.e., −0.03 V).[24e] We suggest that the permeability difference again reflects a disparity in partition coefficients, where the greater hydrophilicity of $Fe(CN)_6^{4-}$ yields a smaller P value. A complimentary explanation, suggested by the reviewers, is that the small shift in oxidation potential specifically reflects differences in the hydrogen bonding environments of the nitrogen atoms of the cyano ligands in water versus the metallopolymeric film. We note that variations in metal-oxidation-dependent ligand/solvent hydrogen bonding interactions (or more generally, Lewis base (CN^-)/Lewis acid (solvent) interactions) result in an extraordinarily large solvent dependence of the formal potential of the ferricyanide/ferrocyanide couple.[29]

Conclusions

The ligand-localized oxidative electropolymerization of $Fe(5\text{-}NH_2\text{-}phen)_3^{2+}$ and $Ru(5\text{-}NH_2\text{-}phen)_3^{2+}$ species in unbuffered aqueous electrolyte solutions yields electrode-supported films that self-limit at thicknesses of ca. 50 and 2 nm, respectively. The films, which are electronically insulating at least over the electrochemical potential range of 0 to +1 V, exhibit highly effective molecular sieving. The evidence for sieving behavior comes from cyclic voltammetry measurements made in solutions containing redox probe molecules of varying effective diameter. Remarkably, even films as thin as ∼2 nm (∼1.5 monolayers) are completely blocking toward large molecular permeants (11 Å diameter), while readily allowing transport of permeants of intermediate size (8 Å). Films obtained via electropolymerization of the metal-free $5\text{-}NH_2$-phen ligand, on the other hand, are impermeable to all but the smallest probe species. Quantitative studies based on rotating disk voltammetry yield transport data that are consistent with a standard membrane diffusion model: For all permeants examined, transport rates vary inversely with metallopolymer film or membrane thickness; i.e., thinner films yield larger rates. Curiously, however, when film thicknesses fall below roughly 10 nm, the trend reverses and transport rates decrease with diminishing film thickness. The chemical and/or structural basis for the reversal has not yet been elucidated.

Acknowledgment. We thank Mr. Jodie L. Conyers for collecting the XPS data.We gratefully acknowledge the Office of Naval Research for financial support. S.B. would also like to acknowledge postdoctoral fellowship support from Le Fonds pour la Formation de Chercheurs et l'Aide à la Recherche (Québec). S.A.M. acknowledges the Northwestern Materials Research Center (NSF-DMR-9632463) for providing a summer undergraduate research fellowship.

LA980908R

(26) For spherical molecules, the Stokes−Einstein equation predicts an inverse relation between D_s and the molecular radius. Furthermore, it has been established (see Koval, C. A.; Ketterer, M. E.; Reidsema, C. M. *J. Phys. Chem.* **1985**, *90*, 4201) that the inverse radius relationship holds reasonably well for nonspherical molecules if the average radius is used. Note that D_f is also presumably inversely proportional to the molecular radius.

(27) Pyati, R.; Murray, R. W. *J. Phys. Chem.* **1994**, *98*, 11129.

(28) The hydrophobic properties of poly-$[Fe(5\text{-}NH_2\text{-}phen)_3^{2+}]$ have previously been studied (in aqueous solution): hydrophobic long-chain alkanesulfonates were shown to partition preferentially over less hydrophobic anions. See: (a) Lyon, L. A.; Ratner, M. A.; Hupp, J. T. *J. Electroanal. Chem.* **1995**, *387*, 109. (b) Ren, X.; Pickup, P. G. *J. Electroanal. Chem.* **1994**, *365*, 289.

(29) See, for example: Gutman, V. *Electrochim. Acta* **1976**, *21*, 661.